

# 000 001 002 003 004 005 006 007 008 009 010 011 012 013 014 015 016 017 018 019 020 021 022 023 024 025 026 027 028 029 030 031 032 033 034 035 CONSISTENT ZERO-SHOT IMITATION WITH CONTRASTIVE GOAL INFERENCE

005 **Anonymous authors**

006 Paper under double-blind review

## ABSTRACT

011 In the same way that generative models today conduct most of their training in  
 012 a self-supervised fashion, how can agentic models conduct their training in a  
 013 self-supervised fashion, interactively exploring, learning, and preparing to quickly  
 014 adapt to new tasks? A prerequisite for embodied agents deployed in real world  
 015 interactions ought to be training with interaction, yet today’s most successful  
 016 AI models (e.g., VLMs, LLMs) are trained without an explicit notion of action.  
 017 The problem of reward-free exploration is well studied in the unsupervised  
 018 reinforcement learning (URL) literature but fails to prepare agents for rapid  
 019 adaptation to new demos. Today’s language and vision models are trained on  
 020 data provided by humans, which provides a strong inductive bias for the sorts of  
 021 tasks that the model will have to solve. However, when prompted to imitate a  
 022 new task, some methods perform distribution matching against the demonstration  
 023 data without properly accounting for the difficulty of various tasks. The key  
 024 contribution of our paper is a method for pre-training interactive agents in a  
 025 self-supervised fashion, so that they can instantly mimic expert demonstrations.  
 026 Our method treats goals (i.e., observations) as the atomic construct. During  
 027 training, our method automatically proposes goals and practices reaching them,  
 028 building off prior work in reinforcement learning exploration. During evaluation,  
 029 our method solves an (amortized) inverse reinforcement learning problem to  
 030 explain demonstrations as optimal goal-reaching behavior. Experiments on  
 031 standard benchmarks (not designed for goal-reaching) show that our approach  
 032 outperforms prior methods for zero-shot imitation.

## 1 INTRODUCTION

034 Today’s AI agents, whether in language or  
 035 robotics, are trained primarily by mimicking  
 036 human demonstrations. But, in the same way  
 037 that children conduct a large degree of learning  
 038 in an unsupervised (adult-free) fashion (Gweon  
 039 & Schulz, 2019; Gopnik, 2020; Stahl & Feigen-  
 040 son, 2015; Poli et al., 2025; Bonawitz et al.,  
 041 2011), how might AI agents develop a foun-  
 042 dation of knowledge through exploration and  
 043 play, rather than through mimicry? In this  
 044 paper, we study the setting where agent pre-  
 045 training is done with no demonstrations, no  
 046 internet-scale data, and no rewards, but rather  
 047 through self-supervised interaction (Agarwal  
 048 et al., 2024; Ma et al., 2022; Wu et al., 2018;  
 049 Eysenbach et al., 2018; Pathak et al., 2017; Mendonca et al., 2021). The agent proposes goals,  
 050 attempts to reach them, and learns from these self-collected data. After training, this agent is assessed  
 051 by its ability to imitate: given a demonstration, the agent uses a (learned) inverse RL module to in-  
 052 fer the demonstrator’s goal, and then uses the (learned) goal-conditioned policies to reach that goal.  
 053 Our problem setting is thus *zero-shot imitation learning (IL)*, where we would like to infer behaviors

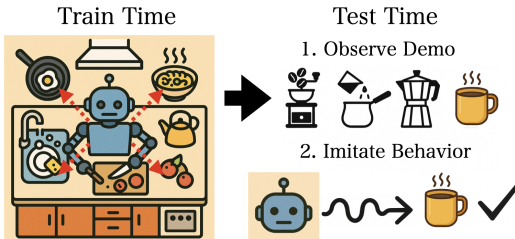


Figure 1: **Zero shot imitation learning.** Assuming access to a multi-task environment, our generalist agent must imagine and practice its own tasks to effectively imitate unknown task demonstrations at test time.

054 from a single demonstration without additional gradient updates (Pirotta et al., 2024; Pathak et al.,  
 055 2018; Jang et al., 2021).

056 It is unclear whether today’s recipe for building generative AI foundation models will be directly  
 057 applicable to *interactive* settings. Though the premise of agents is online exploration or action,  
 058 generative models are primarily built by optimizing self-supervised objectives on input data (Bom-  
 059 masani et al., 2021) collected offline by humans. In robotics, policies are typically constructed  
 060 by either mimicking human demonstrations (Chi et al., 2023; 2024; Octo Model Team et al., 2024;  
 061 Reed et al., 2022) or maximizing human-specified rewards (Silver et al., 2016; Wurman et al., 2022).  
 062 These approaches do have an explicit notion of action, but agents typically practice on a limited set  
 063 of tasks and are not required to infer a demonstrator’s intention. The key idea in our paper is that  
 064 self-supervised pretraining for agentic systems should involve interactive exploration and inverse  
 065 RL that accounts for the relative difficulty of different tasks (Eysenbach et al., 2020; Ziebart et al.,  
 066 2008; Ng & Russell, 2000).

067 Related work in inferring intentions projects a demonstration onto a hypothesis space of reward  
 068 functions and then trains a general-purpose zero-shot RL policy to this space of rewards (Touati &  
 069 Ollivier, 2021; Agarwal et al., 2024; Wu et al., 2018). We make the additional key observation that  
 070 many tasks can be described in terms of goals, such as navigation or manipulation tasks (Brock-  
 071 man et al., 2016). In these settings, goals are described by the agent’s state, and we can imagine  
 072 natural extensions of goals to more complex behaviors expanding the state space. Tasks where the  
 073 necessary actions are more complex or hierarchical, such as cooking a recipe in a kitchen, could  
 074 also be described by a high-dimensional observational state, natural language, or multiple subgoals.  
 075 In addition, maintaining a prior that tasks can be described via goals allows us to define reward  
 076 functions probabilistically in terms of whether we will reach the goal state in the future and apply  
 077 state-of-art goal conditioned reinforcement learning methods (GCRL) to an even further reduced  
 078 hypothesis space of reward functional forms (Kaelbling, 1993; Schaul et al., 2015; Andrychowicz  
 079 et al., 2017). Although this heuristic limits the reward functions we can infer, we show experimen-  
 080 tally that by projecting behavior on the restricted space of goal-conditioned reward functions, we  
 081 can more efficiently summarize and imitate a range of tasks from important benchmarks. Therefore,  
 082 we re-imagine solving the zero-shot imitation learning task by first inferring the expert’s goal and  
 083 then commanding a zero-shot goal-conditioned RL policy to this inferred goal. We start by assess-  
 084 ing our method on goal-reaching tasks, and then evaluate on reward-maximization tasks not tied to  
 085 particular goal states. Our main contributions can be summarized as follows:

- 086 • We propose a contrastive inverse reinforcement learning algorithm (CIRL) for self-  
 087 supervised pretraining of interactive agents that extends contrastive reinforcement learning  
 088 (CRL) methods to the MaxEnt RL setting and includes automatic goal sampling during pre-  
 089 training. Training involves exploration and learning via trial and error, yet requires no demon-  
 090 strations, no rewards, and no preferences.
- 091 • Unlike some structurally similar methods, we prove that our method is consistent: it correctly  
 092 infers the user’s goal using inverse RL, accounting for the relative difficulty of reaching  
 093 different goals.
- 094 • Empirically, we show that our method performs effective autonomous exploration and rapid  
 095 adaptation in the standard URLB benchmark (Laskin et al., 2021), outperforming prior zero-  
 096 shot imitation and zero-shot RL methods.

## 097 2 RELATED WORK

098 We turn to GCRL benchmarks to test our hypotheses for goal-conditioned zero-shot IL. Several  
 099 state-of-art methods on goal-reaching RL use variants of temporally contrastive objectives to learn  
 100 representations and policies, and extend successor feature-based methods to high dimensional envi-  
 101 ronments (Wang et al., 2023; Eysenbach et al., 2022; Myers et al., 2024). However, prior methods  
 102 are limited in their assumption of access to the test-time distribution of goals, focus on the offline  
 103 setting, or a hand-designed exploration policy (Pathak et al., 2018; Eysenbach et al., 2022). Given  
 104 the strength of these methods in RL settings, we naturally ask whether their representations would  
 105 be useful for imitation, and whether we can extend them to also learn to command their own goals.  
 106 We build off the JaxGCRL benchmark to test our ideas with the Contrastive Reinforcement Learning  
 107 (CRL) algorithm on a well-designed suite of tasks (Bortkiewicz et al., 2025).

Our work builds on a rich literature on URL, which use reward-free data to improve performance and generalization of RL algorithms. Some methods focus on extracting reusable representations (Agarwal et al., 2024; Wu et al., 2018; Ghosh et al., 2023; Ma et al., 2022; Blier et al., 2021; Sikchi et al., 2024). However, some of these methods that offer strategies for inferring rewards from demonstrations contain a faulty assumption that matching the expert distribution is sufficient for inferring the demonstrator’s policy without accounting for the partition function over tasks (Touati & Ollivier, 2021; Sikchi et al., 2024). Other works focus on unsupervised discovery of diverse skills (Gregor et al., 2016; Machado et al., 2017; Eysenbach et al., 2018; Sharma et al., 2019; Eysenbach et al., 2021; Klissarov & Machado, 2023; Zahavy et al., 2022; Park et al., 2023a;b; Zheng et al., 2024; Wang et al., 2024). While some of these exhibit zero-shot policy inference capabilities from rewards or goals, they are not designed to perform zero-shot imitation from demonstrations and do not necessarily discover all possible skills (Agarwal et al., 2024; Zheng et al., 2024; Eysenbach et al., 2021). Methods of online unsupervised exploration for pretraining policies tackle problems under similar assumptions as our work, but do not handle zero-shot inference given trajectories (Pathak et al., 2017; 2019; Mendonca et al., 2021; Rajeswar et al., 2022). There has also been significant development of offline unsupervised pre-training methods, but these could suffer under poor exploration and do not focus on the interaction between exploration and policy learning in unfamiliar environments. Our method is highly connected to prior work on learning universal, high dimensional successor representations, with applications to both online and offline settings (Dayan, 1993; Barreto et al., 2016; Borsa et al., 2018; Ma et al., 2018; Touati & Ollivier, 2021; Touati et al., 2022; Pirotta et al., 2024). Like these works, our method contains an inductive bias influencing which tasks we focus on, namely those that are goal-reaching. We show that this restriction becomes particularly useful for inverse RL, even for arbitrary reward functions.

Approaches to zero-shot imitation learning combine approaches to inverse RL and exploration/data collection to solve the problem. We’ll discuss these individual components first and then discuss key prior methods for zero-shot imitation.

**Inverse RL** Achieving general, adaptable agents is challenging via reward engineering and may lead to unintended behaviors (Amodei et al., 2016). Thus, we turn to learning from demonstrations (LfD), assuming we have access to limited data from an expert (Finn et al., 2016; Fu et al., 2018; Pirotta et al., 2024; Yu et al., 2019). The main approaches to LfD are behavioral cloning (BC) and inverse reinforcement learning (IRL). BC casts learning an imitation policy as a supervised learning problem. While BC can work well in practice, it suffers from poor performance under distributional shift and can overfit its expert demonstrations (Ross et al., 2011; Pomerleau, 1988; Bojarski et al., 2016). IRL attempts to infer reward functions/corresponding policies from demonstrations (Ng & Russell, 2000). Since the reward inference problem is inherently under-specified, a common modeling choice is the Maximum Entropy assumption, which assumes that expert demonstrations select actions to maximize both the sum of expected discounted rewards and the entropy of the distribution of actions over states (Ziebart et al., 2008). Extensions such as GAIL, AIRL, and GCL were developed to use deep function approximators for single-task IRL (Ho & Ermon, 2016; Fu et al., 2018; Finn et al., 2016). Current multi-task/meta IL algorithms can be categorized as gradient-based or context-based (Chen et al., 2023). Gradient-based approaches, such as (Finn et al., 2017; Yu et al., 2018) combine meta-learning with IL to recover a policy, but at inference time, require a one-shot gradient step to adapt to a new task whereas our method adapts zero-shot. Context-based approaches such as SMILE and PEMIRL learn a latent variable to represent the task contexts and train a context-conditioned policy that can be applied zero-shot to new tasks (Seyed Ghasemipour et al., 2019; Yu et al., 2019). Our approach is similar (encoding goals as a form of context) but takes this one step further by proving that the multi-task IRL problem can actually be reduced to a purely goal-inference problem when we our expert optimizes a goal-conditioned reward function. Therefore, we can use zero-shot RL algorithms to recover policies without loss of performance instead of using less stable adversarial methods.

**Exploration** While BC and IRL can be performed on offline datasets, we would prefer to enable zero-shot imitation through purely online methods that can be applied out-of-the-box in novel environments. This requires our IL agent to perform its own exploration, which CRL currently does not support (Eysenbach et al., 2022). For our goal-conditioned setting, automatic goal sampling enables us to autonomously generate training objectives. Goal sampling approaches broadly fall into two categories: adversarial methods and distribution-based methods. Adversarial methods such as

162 ASP and GoalGAN introduce a second policy for sampling goals (OpenAI et al., 2021; Florensa  
 163 et al., 2018). While effective for simple domains, these methods can struggle with high-dimensional  
 164 goal spaces and require careful balancing of the adversarial training process. State distribution  
 165 approximation methods such as Skew-Fit, EDL, VUVC, RIG, MEGA, and DISCERN control the  
 166 probability of selecting a goal via the empirical state visitation density, usually trying to cover the  
 167 full state space with exploration (Pong et al., 2020; Campos et al., 2020; Kim et al., 2023; Nair et al.,  
 168 2018; Pitis et al., 2020; Warde-Farley et al., 2018). Our method, GoalKDE, adopts a simple form of  
 169 RIG, although more complex methods could also be benchmarked in future work.  
 170

171 **Zero-Shot Imitation Learning** BC-Zero addresses multi-task zero-shot imitation by scaling di-  
 172 verse, human-in-the-loop data collection and training a single task-conditioned behavior-cloned  
 173 policy that can execute novel text instructions at test time (Jang et al., 2021). However, unlike  
 174 our method, BC-Zero gathers task-labelled expert data via teleoperation and requires human in-  
 175 terventions in a DAgger-style loop, whereas our method trains purely online and collects its own  
 176 data using a self-supervised objective and exploration. Zero-Shot Visual Imitation uses goal-  
 177 conditioned policies to imitate experts trained via a model-based forward consistency loss (Pathak  
 178 et al., 2018). However, unlike our work, they hand-devised an exploration policy to generate data for  
 179 model-based training, whereas our data collection is fully self-supervised for model-free training.  
 180 Forward-Backward (FB) Representations and RLZero enable zero-shot imitation through matching  
 181 the demonstrator’s state visitation distributions (Touati & Ollivier, 2021; Pirotta et al., 2024; Sikchi  
 182 et al., 2024). However, we prove for the FB representation that without accounting for the partition  
 183 function, this method leads to systematic misidentification of the demonstrator’s true policy.  
 184

### 3 PRELIMINARIES

187 **Definition 1.** *The zero-shot imitation learning problem assumes we are given a single expert tra-  
 188 jectory  $\tau = (s_0, a_0, \dots, s_T, a_T)$  at inference time, generated by some unknown expert policy  $\pi_E$   
 189 with trajectory distribution  $p_{\pi_E}(\tau)$ . No reward function is available. We must produce a policy  
 190  $\hat{\pi}_{CIRL} \in \Pi$  that successfully reproduces the behavior of  $\pi_E$  defined by its unknown reward function,  
 191 thereby achieving low regret.  $\hat{\pi}_{CIRL}$  should be inferred from  $\pi_E$  with no additional environment in-  
 192 teraction, test-time data, or gradient updates.*

193 To solve this problem, we will model the environment as a goal-conditioned MDP, defining a reward  
 194 function that depends on a goal and thereby assuming that expert policies  $\pi_E$  have behaviors that can  
 195 be described as goal-reaching. Then, we can infer the reward function associated with  $\pi_E$  via Max-  
 196 Ent IRL. To do this, we will infer the goal  $\hat{g}$  associated with  $\pi_E$ , and command a goal-conditioned  
 197 policy to  $\hat{g}$  that is trained with CRL. In the subsequent sections, we will prove that performing Max-  
 198 Ent IRL with a goal-conditioned reward is equivalent to performing goal inference. We operate  
 199 in the pure online RL setting, assuming no access to offline expert data during pretraining. This  
 200 includes no access to the test-time goal distribution, a departure from CRL’s oracle assumptions.  
 201

#### 3.1 CONTRASTIVE RL

202 We define a goal-conditioned MDP by a tuple  $(S, A, G, P, r, \rho)$ , where  $S$  is the state space,  $A$  is the  
 203 action space,  $G$  is the goal space (equivalent to the state space in our formulation);  $p : S \times A \times S \rightarrow [0, 1]$  describes the transition probabilities between states;  $r : S \times A \times G \rightarrow \mathbb{R}$  is a goal-  
 204 conditioned reward function, defined as  $r(s_t, a_t, g) = (1 - \gamma)p(s_{t+1} = s_g | s_t, a_t) = r_g(s_t, a_t)$ ,  
 205 for some discount factor  $\gamma$ ;  $\rho_0(s_0)$  specifies the initial state distribution, and  $p(g)$  specifies some  
 206 test-time distribution over goals. We use  $\tau$  to define a finite horizon trajectory as a sequence of  
 207 states and actions:  $\tau = (s_0, a_0, \dots, s_T, a_T)$ , and write the likelihood of a trajectory under policy  
 208  $\pi$  as  $p(\tau) = \rho_0(s_0) \prod_t p(s_{t+1} | s_t, a_t) \pi(a_t | s_t)$ . We also define the discounted future state  $s_f$   
 209 occupancy measure (density) of goal-conditioned policy  $\pi : S \times G \rightarrow \Delta(\mathcal{A})$  as  $p_\gamma^\pi(s_f | s, a, g) =$   
 210  $(1 - \gamma) \sum_{t=0}^{\infty} \gamma^t p_t^\pi(s_t | s, a, g)$  and the marginal distribution as  $p_\gamma^\beta(s_f) = \int p^\beta(s, a) p_G(g) p_\gamma^\beta(s_f |$   
 211  $s, a, g) ds da dg$ , where  $\beta : S \rightarrow \mathcal{A}$  is the behavioral policy. Using the contrastive RL algorithm,  
 212 we can estimate the discounted state occupancy using Noise Contrastive Estimation (Oord et al.,  
 213 2018) and obtain the critic function  $f_{\phi, \psi}^*(s, a, g) = \|\phi(s, a) - \psi(g)\|_2 = \log \frac{p_\gamma^\pi(s_f | s, a, g)}{p_\gamma^\beta(s_f)} = \frac{1}{p_\gamma^\beta(s_f)}$ .  
 214

216  $Q_{sf}^{\pi(\cdot| \cdot)}(s, a)$ , where  $Q_{sf}^{\pi}(s, a) \triangleq \mathbb{E}_{\pi(\tau|s_f)} \left[ \sum_{t'=t}^{\infty} \gamma^{t'-t} r_{sf}(s_{t'}, a_{t'}) \mid s_t = s, a_t = a \right]$  (Eysenbach  
217 et al., 2022).  
218

219 3.2 MAXIMUM ENTROPY INVERSE REINFORCEMENT LEARNING (MAXENT IRL)  
220

221 We will use the MaxEnt IRL framework to infer reward functions and policies from ex-  
222 pert demonstrations. This framework assumes that demonstrations come from a MaxEnt  
223 RL policy  $\tilde{\pi}^* = \arg \max_{\pi} \mathbb{E}_{\tau \sim \pi} \left[ \sum_{t=0}^T (r_g(s_t, a_t) + \alpha \mathcal{H}(\pi(\cdot|s_t))) \right]$  where  $\alpha$  is an op-  
224 tional parameter to control the trade-off between reward maximization and entropy max-  
225 imization. Without loss of generality, we can assume  $\alpha = 1$  for notational sim-  
226 plicity. The trajectory likelihood under the optimal maximum entropy policy is then  
227  $p^*(\tau = \{s_{0:T}, a_{0:T}\} \mid g) = \frac{1}{Z_g} \left[ \rho_0(s_0) \prod_{t=0}^T p(s_{t+1} \mid s_t, a_t) \right] \exp \left( \sum_{t=0}^T r_g(s_t, a_t) \right)$ , where  
228  $Z_g = \int \rho(s_0) \prod_{t=0}^T P(s_{t+1} \mid s_t, a_t) e^{r_g(s_t, a_t)} d\tau$ . We can then define the MaxEnt IRL problem as  
229  $\min_{g'} \mathbb{E}_{p(g)} [D_{\text{KL}}(p_E(\tau|g) \parallel p^*(\tau = \{s_{0:T}, a_{0:T}\} \mid g'))]$ .  
230

231 3.3 GOAL INFERENCE  
232

233 The MaxEnt IRL problem involves inferring reward parameters from a demonstration, and our re-  
234 ward functions are completely parameterized by goals  $g$ . Therefore, we will perform inference to  
235 recover the latent goal of an actor from observed data. Applying Bayes' Rule to the trajectory like-  
236 lihood of a MaxEnt RL policy, the posterior distribution over goals is  $p^*(g \mid \tau) = \frac{p^*(\tau|g)p(g)}{p(\tau)} \propto$   
237  $p(g)e^{\sum_t r_g(s_t, a_t) - \log Z_g}$ . The partition function  $Z_g$  is important for inferring goals, since it gives  
238 us a notion of average reward collected along all possible trajectories for a given reward function  
239  $r_g(s, a)$ . If an expert demonstration collects more reward than this average over trajectories, it is  
240 more likely that the demonstration is associated with this particular goal (Eysenbach et al., 2020).  
241 The partition function is difficult to estimate, so we will instead fit a variational posterior  $q_{\xi}(g|\tau)$  to  
242 perform goal inference (Dragan et al., 2013; Zurek et al., 2021).  
243

244 4 METHOD  
245

246 Our algorithm, CIRL, consists of the following components: (1) self-supervised contrastive RL  
247 pretraining to learn maximum entropy soft Q-values and a corresponding goal conditioned policy,  
248 (2) a goal inference model to learn the variational posterior, and (3) automatic goal sampling during  
249 pretraining. Our key contribution is in using goal inference and a goal-conditioned reward to couple  
250 IRL with CRL for a successful online imitation learning algorithm. However, certain components,  
251 such as the specific goal sampling method, could be substituted.  
252

253 4.1 MAXIMUM ENTROPY CONTRASTIVE REINFORCEMENT LEARNING  
254

255 We build an extension of contrastive reinforcement learning under the Maximum Entropy assumption.  
256 While CRL just learns the sum of discounted future rewards, we also need to estimate the sum  
257 of discounted future entropy to optimize the MaxEnt RL objective. Following prior work (Haarnoja  
258 et al., 2018; Eysenbach et al., 2022), we define the the entropy regularized goal-conditioned reward  
259 function as  $\tilde{r}_g(s_t, a_t) \triangleq (1 - \gamma)\delta(s_t = g) - \alpha \log \pi(a \mid s, g)$ , where  $\delta(\cdot = g)$  is the delta  
260 measure at the goal  $g$ . Given a set of goals sampled from a goal distribution  $g \sim p_G(g)$ , this new  
261 reward function allows us to rewrite the objective of the goal-conditioned policy as maximizing the  
262 entropy-regularized discounted state occupancy measure:  $\max_{\pi} \mathcal{L}_{\text{Actor}}(\pi)$ ,  
263

$$\mathcal{L}_{\text{Actor}}(\pi) = \mathbb{E}_{g \sim p_G(g), \tau \sim \pi(\tau|g)} \left[ (1 - \gamma) \sum_{t=0}^{\infty} \gamma^t (r_g(s, a) - \alpha \log \pi(a \mid s, g)) \right] \quad (1)$$

$$= \mathbb{E}_{\substack{g \sim p_G(g), s \sim \rho(s), a \sim \pi(a|s, g), \\ s_f \sim p_{\gamma}^{\pi}(s_f=g|s, a, g), a_f \sim \pi(a_f|s_f, g)}} [\delta(s_f = g) - \alpha \log \pi(a_f \mid s_f, g)] \quad (2)$$

$$\approx \mathbb{E}_{g \sim p_G(g), s \sim p^{\beta}(s), a \sim \pi(a|s, g)} [\exp(f_{\phi, \psi}(s, a, g)) - \alpha \log \pi(a \mid s, g)] = \tilde{Q}_g(s, a) \quad (3)$$

270 Thus, we augment CRL to optimize the soft Q function  $\tilde{Q}_g(s, a)$  by optimizing the CRL loss  
 271  $\min_{\phi, \psi} \mathcal{L}_{\text{Critic}}(\phi, \psi)$ , where  
 272

273  $\mathcal{L}_{\text{Critic}}(\phi, \psi) = \mathbb{E}_{\mathcal{B}} \left[ -\sum_{i=1}^{|\mathcal{B}|} \log \left( \frac{e^{f_{\phi, \psi}(s_i, a_i, g_i)}}{\sum_{j=1}^K e^{f_{\phi, \psi}(s_i, a_i, g_j)}} \right) - \sum_{i=1}^{|\mathcal{B}|} \log \left( \frac{e^{f_{\phi, \psi}(s_i, a_i, g_i)}}{\sum_{j=1}^K e^{f_{\phi, \psi}(s_j, a_j, g_i)}} \right) \right]$  for  
 274  $\left\{ f_{\phi, \psi}(s_i, a_i, g_j) \right\}_{i,j}$  over the elements of the batch  $\mathcal{B}$  (Bortkiewicz et al., 2025). The critic function  
 275  $f_{\phi, \psi}(s, a, g)$  estimates expected discounted future state occupancy, and the actor objective combines  
 276 this with an additional term  $\mathcal{L}_{\text{Entropy}}(\theta) = -\mathbb{E}_{g \sim p_{\mathcal{G}}(g), \tau \sim \pi(\tau|g)} [(1 - \gamma) \sum_{t=0}^{\infty} \gamma^t (\alpha \log \pi(a | s, g))]$   
 277 that estimates expected discounted future entropy. This term will be optimized with temporal differ-  
 278 ence updates. See Appendix B for more details on the algorithm.  
 279

## 281 4.2 VARIATIONAL GOAL INFERENCE

283 Following the motivation of Section 3.3, we will learn a variational distribution  $q_{\xi}(g|\tau)$  to match  
 284 the true posterior  $p^*(g|\tau)$ . We optimize the forward KL objective to achieve this (Ambrogioni  
 285 et al., 2019; Yu et al., 2019):  $\min_{\xi} D_{KL}(p^*(g | \tau) \| q_{\xi}(g | \tau)) = \min_{\xi} \mathbb{E}_{p^*(g, \tau)} \left[ \log \frac{p^*(g | \tau)}{q_{\xi}(g | \tau)} \right] =$   
 286  $\max_{\xi} \mathbb{E}_{g \sim p(g); \tau \sim p^*(\tau|g)} [\log q_{\xi}(g | \tau)] = \max_{\xi} \mathcal{L}_{\text{Info}}(\xi)$ .  
 287

288 When our policy is trained to optimality, it will emit a trajectory distribution equivalent to  $p^*(\tau|g)$ .  
 289 Thus, we can use our online learned MaxEnt RL policy to sample trajectories both for contrastive  
 290 RL pre-training and for learning the variational posterior.

291 Another way to model the variational posterior is with the mean field approximation:  $q_{\xi}(g|\tau) =$   
 292  $\prod_{t=0}^T q_{\xi}(g|s_t, a_t)$ , where each local state-action independently influences the distribution over the  
 293 goal. This form can be much easier to train since parameters  $\xi$  are now shared across state-  
 294 action inputs. We can rewrite the expression for the true posterior as  $p^*(g | \tau) = \frac{p^*(\tau|g)p(g)}{p(\tau)} \propto$   
 295  $p(g)e^{\sum_{t=0}^T r_{\theta}(s_t, a_t, g) - \frac{1}{T} \log Z_{\theta}} \propto \prod_{t=0}^T e^{r_{\theta}(s_t, a_t, g) - \frac{1}{T} Z_{\theta}}$ , and note that it precisely takes a mean  
 296 field form when the input trajectory is finite. Thus, we can establish a corollary to motivate the use  
 297 of the mean field approximation when optimizing  $\mathcal{L}_{\text{Info}}(\xi)$  for our method, training a Gaussian MLP  
 298 to perform amortized variational inference with the mean field approximation.  
 299

300 **Corollary 1.** *Without loss of generality, the class of mean field goal inference models includes the*  
 301 *true posterior distribution.*

## 302 4.3 CIRL IS CONSISTENT

304 Our main theoretical result is to show that our method infers the correct distribution over expert  
 305 goals. This statement is non-trivial because the most-frequented states may not be the user’s in-  
 306 tended state, so correctly performing goal inference requires reasoning about the relative difficulty  
 307 of different goals. Proof can be found in Appendix A.1.

308 **Lemma 1.** *Let policy  $\pi_{\text{demo}}$  be given. CIRL produces policy  $\pi_{\text{CIRL}}$  that consistently*  
 309 *infers rewards by converting the MaxEnt IRL problem into a goal inference problem:*  
 310  $\min_{\theta} \mathbb{E}_{p(g)} [D_{KL}(p_E(\tau|g) \| p^*(\tau|g))] \implies \max_{\xi} \mathbb{E}_{g \sim p(g); \tau \sim p^*(\tau|g)} [\log q_{\xi}(g | \tau)]$   
 311

312 **IRL with FB is Inconsistent** FB (Touati & Ollivier, 2021) is presented as a method that can learn  
 313 optimal policies for any task and proposes to imitate trajectories by inferring their reward and then  
 314 using the corresponding reward-maximizing policy. In this section, we show that even if FB learns  
 315 optimal policies for every reward function, it doesn’t correctly identify which reward function a  
 316 demonstrator is maximizing, thereby provably failing to perform zero-shot imitation. Proof can be  
 317 found in Appendix A.2.

318 **Lemma 2.** *There exists an MDP with two unique reward-maximizing policies  $(\pi_1, \pi_2)$ , where FB*  
 319 *incorrectly demonstrates policy  $\pi_1$  with policy  $\pi_2$ .*

## 321 4.4 GOAL-SAMPLING

323 During training, we use states stored in the replay buffer to continually fit a Gaussian Kernel Density  
 324 estimator (KDE) approximating the distribution of visited states. This buffer is pre-filled at the start

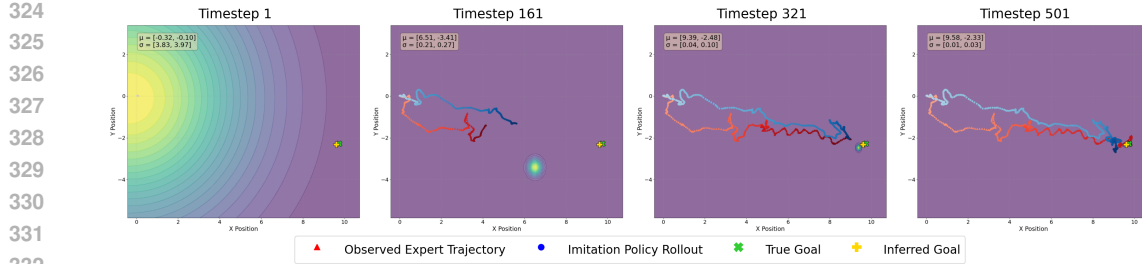


Figure 2: **Zero-shot imitation learning with CIRL via goal inference.** CIRL combines goal-conditioned contrastive RL pre-training, automatic goal sampling for exploration, and a mean field goal inference model to imitate expert demonstrations. Here we see how an Ant’s imitation policy and posterior distribution over goal states evolve across timesteps toward a final maximum a posteriori (MAP) estimate.

of training with data from a randomly initialized policy, and at each iteration, we select the state from the buffer that has the lowest probability under the KDE to train the policy. We call this method of automatic exploration: GoalKDE. See Appendix B for a summary of the full CIRL algorithm.

## 5 EXPERIMENTS

Our method contains components for self-supervised RL pretraining, automatic goal sampling, and goal inference. We ablate each in turn, and show that CIRL (CRL Pre-training + GoalKDE Exploration + Mean Field Goal Inference Model) can learn good representations for imitation across several environments. We use the JaxGCRL and Unsupervised Reinforcement Learning Benchmark (URLB) environments (Bortkiewicz et al., 2025; Laskin et al., 2021). Details are provided in Appendix C.

For our evaluation, we train an expert policy using CRL under oracle goal sampling. Using this policy, we sample 2000 goals from the oracle test distribution of goals and unroll the CRL expert policy toward each goal. For each expert demonstration, we perform zero-shot IL across our ablation setup, reporting imitation score (the ratio between the cumulative return of the algorithm and the average cumulative reward of the expert) (Pirrotta et al., 2024). Unless otherwise noted, all methods were trained online. The only exceptions are FB (Offline) and goal-conditioned behavioral cloning (GCBC), which use the CRL expert policy data. FB (Offline) uses 2000 distinct trajectories of 1025 steps each sampled from the CRL expert policy. GCBC trains a goal-conditioned policy with the same number of update steps as the CRL expert. We also further evaluate using non-goal-conditioned policy demonstrations trained with URLB rewards on the Ant Forward, Ant Jump, and Ant Flip tasks and demonstrate the capability of CIRL to imitate these policies with low regret.

### 5.1 CIRL w/ SELF-SUPERVISED PRETRAINING OUTPERFORMS BASELINES

We first compare CIRL against several baselines for imitation learning, including those with and without access to expert data during training. For each environment, we compared the reward earned by an expert policy (CRL) and the imitation learning method, reporting the fraction of expert reward achieved as the “imitation score.” The baselines, both trained with no access to expert information, include the Nearest Neighbor baseline, which in a given state considers the 1-NN state in the expert demonstration and applies its corresponding action. We also include the URL baselines of FB representation (Touati & Ollivier, 2021), PSM (Agarwal et al., 2024), and HILP (Wu et al., 2018). The inferred latents for these methods were computed from expert demonstration states (Pirrotta et al., 2024). As seen in Figure 3, CIRL consistently outperforms all baselines, regardless of en-

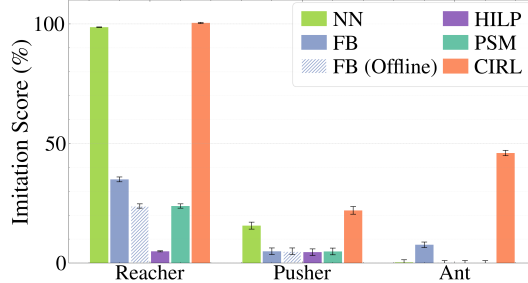


Figure 3: **Value of self-supervised RL pre-training** CIRL consistently outperforms the alternative FB representation zero-shot imitation method as well as the naive 1-NN policy baseline.

For our evaluation, we train an expert policy using CRL under oracle goal sampling. Using this policy, we sample 2000 goals from the oracle test distribution of goals and unroll the CRL expert policy toward each goal. For each expert demonstration, we perform zero-shot IL across our ablation setup, reporting imitation score (the ratio between the cumulative return of the algorithm and the average cumulative reward of the expert) (Pirrotta et al., 2024). Unless otherwise noted, all methods were trained online. The only exceptions are FB (Offline) and goal-conditioned behavioral cloning (GCBC), which use the CRL expert policy data. FB (Offline) uses 2000 distinct trajectories of 1025 steps each sampled from the CRL expert policy. GCBC trains a goal-conditioned policy with the same number of update steps as the CRL expert. We also further evaluate using non-goal-conditioned policy demonstrations trained with URLB rewards on the Ant Forward, Ant Jump, and Ant Flip tasks and demonstrate the capability of CIRL to imitate these policies with low regret.

378  
 379  
 380  
 381  
 382  
 383  
 384  
 385  
 386  
 387  
 388  
 389  
 390  
 391  
 392  
 393  
 394  
 395  
 396  
 397  
 398  
 399  
 400  
 401  
 402  
 403  
 404  
 405  
 406  
 407  
 408  
 409  
 410  
 411  
 412  
 413  
 414  
 415  
 416  
 417  
 418  
 419  
 420  
 421  
 422  
 423  
 424  
 425  
 426  
 427  
 428  
 429  
 430  
 431  
 vironment difficulty, making it the most promising technique for learning to imitate in unfamiliar goal-conditioned environments. Even if we train the FB representation with data from the expert policy, this baseline is unable to achieve comparable imitation scores to our method.

## 5.2 CIRL PRE-TRAINING OUTPERFORMS THE FB REPRESENTATION

CIRL and FB representation’s algorithms have two main structural differences: the way it learns the successor representation and the way it infers intentions. To better understand why CIRL outperforms the FB representation, we hold the method of inferring intentions constant and only use information from the last state of the expert demonstration. Note that for tasks where the goal state is transient (e.g. tossing a ball to reach a particular height), the last state in a trajectory may not contain enough information about the true goal, but for Ant, Reacher, and Pusher, the agents are able to reach and stay at all possible goals. As seen in Figure 4, FB only achieves a small fraction of the imitation score of CIRL under these conditions. This result provides evidence that learning reward functions is indeed more expressive than summarizing behavior via goals, as it is easier for CIRL to learn a successor representation for reaching goals than it is for FB to learn more general reward functions. Additionally, in Figure 9 in Appendix D, even if we instead use the CIRL inferred goal to compute a latent for the FB representation, we are still not able to match CIRL’s performance, though performance does improve compared to using the averaged backward representation of the entire demonstration or the backward representation of the last state.

## 5.3 MEAN FIELD APPROXIMATION IMPROVES GOAL INFERENCE

Our theory suggests that inferring goals using a mean field approximation should preserve predictive power compared to using the full  $\tau$  as input to the context encoder. We also have fewer parameters to train under the mean field assumption, and thus hypothesize that it will outperform the full  $\tau$  alternative. Testing this across environments with CIRL and GCBC, in Figure 5, we see that mean field goal inference universally outperforms the alternative of inferring goals, regardless of environment or training algorithm. These experiments validate our corollary of the preserved predictive power of mean field goal inference, with the added computational benefits of this simplified modeling choice. The mean field assumption also allows us to reliably infer goals from partial trajectories, as shown in Figure 2, where we see the posterior distribution hone in on the true goal as the imitator observes more of the demonstration.

## 5.4 BETTER AUTOMATIC GOAL SAMPLING IMPROVES IMITATION SCORES

While we see that CIRL with GoalKDE automatic goal sampling outperforms our baselines with no expert data, we ablate our GoalKDE goal sampling method against oracle goal sampling (which

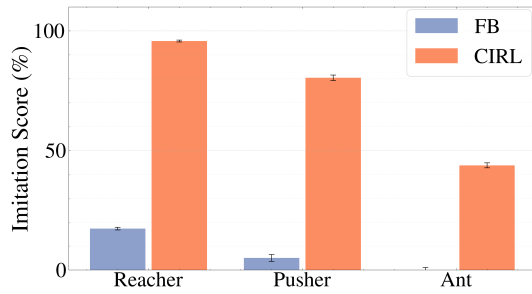


Figure 4: **Summarizing behavior via goals yields better imitation than reward-based explanations.** When using the last expert demonstration state as the goal, CIRL achieves high imitation scores on goal-conditioned environments while FB struggles to infer goal-conditioned reward functions from online learning.

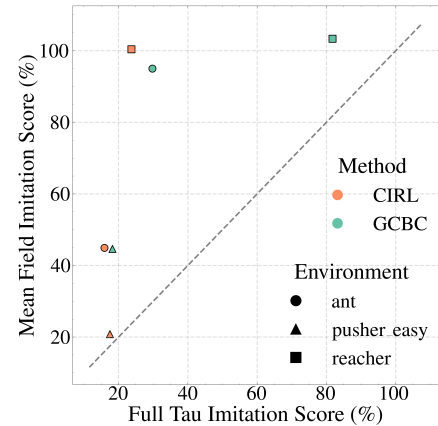


Figure 5: **Mean field goal inference models outperform alternative full  $\tau$  input models.** The mean field model (CIRL and GCBC) consistently outperforms the full  $\tau$  model (reacher, pusher easy, ant) across all environments.

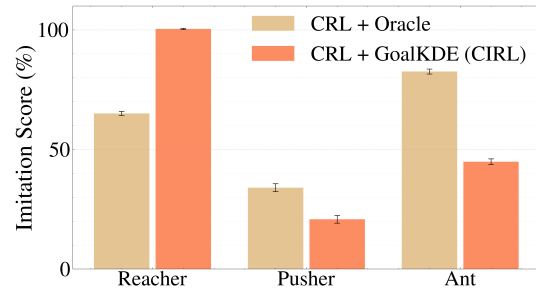
432 trains CRL on the test-time goal distribution) to experimentally quantify the gap between these  
 433 methods. We see in Figure 6 that in the Reacher environment, training CRL policies with GoalKDE  
 434 can yield near-perfect imitation scores, and that sometimes GoalKDE can better explore the state  
 435 space for more generalizable policies. However, for the higher dimensional state spaces in Ant and  
 436 Pusher, a combination of more sophisticated goal sampling techniques or more training steps on  
 437 more automatically sampled goals could boost performance beyond oracle sampling. See Figure 8  
 438 in Appendix D for additional results ablating the CIRL goal inference method as well as Figure 10  
 439 for analysis of limitations of GoalKDE in increasingly complex PointMaze environments.

### 440 441 5.5 CIRL SUPPORTS IMITATION BEYOND GOAL-CONDITIONED ENVIRONMENTS

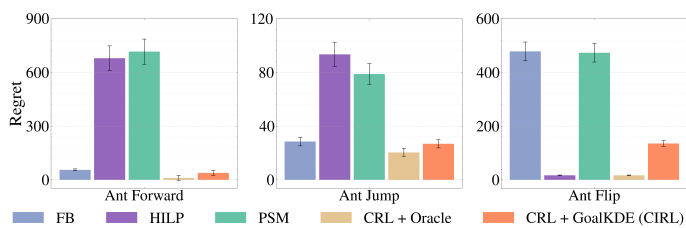
442 We run further experiments on the standard  
 443 URLB benchmark, which is not designed for  
 444 goal-reaching, to show that CIRL outperforms  
 445 prior methods for zero-shot imitation when im-  
 446 itating policies (1) trained with more general  
 447 reward functions and (2) which require ex-  
 448 panding the goal hypothesis space. Following  
 449 the URLB Benchmark, we train expert poli-  
 450 cies on the Ant Forward, Ant Jump, and Ant  
 451 Flip tasks with PPO on non-goal-conditioned  
 452 reward functions, and report regret of CIRL in-  
 453 ferred policies compared to these expert poli-  
 454 cies. We see in Figure 7 that CRL pre-training  
 455 methods can achieve lower regret than FB,  
 456 HILP, or PSM imitation policies by inferring  
 457 goals involving the ant’s torso 3D position and  
 458 linear/angular velocity. CRL + Oracle goal  
 459 sampling could perform better in some environ-  
 460 ments due to sampling fewer infeasible goals,  
 461 and extensions to CIRL’s exploration scheme based on related work could overcome this difficulty  
 462 (OpenAI et al., 2021). Thus, CIRL can scale to more complex reward functions as long as we  
 463 sufficiently expand the goal space to capture the task.

## 464 6 LIMITATIONS AND CONCLUSION

466 Since not all reward functions  
 467 are goal reaching, future work  
 468 could close the gap between  
 469 these reward hypothesis classes  
 470 by exploring richer goal repre-  
 471 sentations, such as language  
 472 or multi-modal spaces, and  
 473 consider summarizing behavior  
 474 with multiple sub-goals. Our  
 475 method also requires access to a  
 476 simulator and would require fur-  
 477 ther research to evaluate appli-  
 478 cability in safety-critical settings, settings where collecting data is prohibitively expensive, or human  
 479 interaction settings. With more complex goal spaces, related work in exploration could be applied  
 480 as a substitute for our GoalKDE method. A full comparison of goal-sampling methods is outside  
 481 of the scope of this paper. Our main aim is to propose a full pipeline for enabling imitation via an  
 482 imagine-and-practice loop in the complete absence of expert data. We introduced a framework for  
 483 goal-conditioned maximum entropy inverse reinforcement learning that leverages self-supervised  
 484 contrastive RL pretraining, automatic goal sampling, and a mean field variational goal inference  
 485 model to enable zero-shot imitation from a single demonstration without access to an offline expert  
 data during training. By re-framing reward inference as goal state inference and coupling this with  
 CRL, our method learns transferable policies across diverse task distributions.



464 **Figure 6: GoalKDE exploration vs. oracle goal  
 465 sampling during CRL pre-training.** Holding  
 466 the goal inference method constant (mean field  
 467 inference), we find that GoalKDE sampling can  
 468 achieve a significant fraction of imitation score  
 469 compared to the oracle baseline, and can even out-  
 470 perform this baseline in some environments.



464 **Figure 7: CIRL inferred goals efficiently summarize complex  
 465 rewards.** CIRL achieves lower regret than FB when imitating  
 466 URLB policies with non-goal-reaching rewards.

486 7 REPRODUCIBILITY STATEMENT  
487488 All experiments in this paper are completely reproducible by running the experiments in our code:  
489 <https://anonymous.4open.science/r/cirl-3CD7/README.md>. Background information  
490 on the environments used and algorithm implementations can be found in the Appendix, and any-  
491 thing not noted can be assumed to follow the defaults of the JaxGCRL and URLB benchmarks  
492 (Bortkiewicz et al., 2025; Laskin et al., 2021). Our method is based on open source Brax (Freeman  
493 et al., 2021) and Jax (Bradbury et al., 2018) libraries. We also used LLMs in completing this work  
494 for two purposes: to polish the paper, including generating some of the icons used in Figure 1 and  
495 for the additional purpose of aiding in code writing (via the Cursor AI application).496 REFERENCES  
497498 Siddhant Agarwal, Harshit S. Sikchi, Peter Stone, and Amy Zhang. Proto successor measure: Rep-  
499 resenting the space of all possible solutions of reinforcement learning. *ArXiv*, abs/2411.19418,  
500 2024. URL <https://api.semanticscholar.org/CorpusID:274423014>.  
501  
502 Luca Ambrogioni, Umut Güçlü, Julia Berezutskaya, Eva van den Borne, Yağmur Güçlütürk, Max  
503 Hinne, Eric Maris, and Marcel van Gerven. Forward amortized inference for likelihood-free  
504 variational marginalization. In Kamalika Chaudhuri and Masashi Sugiyama (eds.), *Proceedings*  
505 *of the Twenty-Second International Conference on Artificial Intelligence and Statistics*, volume 89  
506 *of Proceedings of Machine Learning Research*, pp. 777–786. PMLR, 16–18 Apr 2019. URL  
507 <https://proceedings.mlr.press/v89/ambrogioni19a.html>.  
508 Dario Amodei, Chris Olah, Jacob Steinhardt, Paul Francis Christiano, John Schulman, and Dan-  
509 delion Mané. Concrete problems in ai safety. *ArXiv*, abs/1606.06565, 2016. URL <https://api.semanticscholar.org/CorpusID:10242377>.  
510  
511 Marcin Andrychowicz, Filip Wolski, Alex Ray, Jonas Schneider, Rachel Fong, Peter Welinder,  
512 Bob McGrew, Josh Tobin, OpenAI Pieter Abbeel, and Wojciech Zaremba. Hindsight experi-  
513 ence replay. In I. Guyon, U. Von Luxburg, S. Bengio, H. Wallach, R. Fergus, S. Vishwanathan,  
514 and R. Garnett (eds.), *Advances in Neural Information Processing Systems*, volume 30. Cur-  
515 ran Associates, Inc., 2017. URL [https://proceedings.neurips.cc/paper\\_files/paper/2017/file/453fadbd8a1a3af50a9df4df899537b5-Paper.pdf](https://proceedings.neurips.cc/paper_files/paper/2017/file/453fadbd8a1a3af50a9df4df899537b5-Paper.pdf).  
516  
517 André Barreto, Will Dabney, R Munos, Jonathan J Hunt, T Schaul, David Silver, and H V  
518 Hasselt. Successor features for transfer in reinforcement learning. *Neural Inf Process Syst*,  
519 abs/1606.05312, June 2016.  
520  
521 Léonard Blier, Corentin Tallec, and Yann Ollivier. Learning successor states and goal-dependent  
522 values: A mathematical viewpoint. *ArXiv*, abs/2101.07123, 2021. URL <https://api.semanticscholar.org/CorpusID:231632451>.  
523  
524 Mariusz Bojarski, Davide Del Testa, Daniel Dworakowski, Bernhard Firner, Beat Flepp, Prasoon  
525 Goyal, Lawrence D Jackel, Mathew Monfort, Urs Muller, Jiakai Zhang, Xin Zhang, Jake Zhao,  
526 and Karol Zieba. End to end learning for self-driving cars. *arXiv [cs.CV]*, April 2016.  
527  
528 Rishi Bommasani, Drew A. Hudson, Ehsan Adeli, Russ Altman, Simran Arora, Sydney von Arx,  
529 Michael S. Bernstein, Jeannette Bohg, Antoine Bosselut, Emma Brunskill, Erik Brynjolfsson,  
530 S. Buch, Dallas Card, Rodrigo Castellon, Niladri S. Chatterji, Annie S. Chen, Kathleen A. Creel,  
531 Jared Davis, Dora Demszky, Chris Donahue, Moussa Doumbouya, Esin Durmus, Stefano Ermon,  
532 John Etchemendy, Kawin Ethayarajh, Li Fei-Fei, Chelsea Finn, Trevor Gale, Lauren E. Gillespie,  
533 Karan Goel, Noah D. Goodman, Shelby Grossman, Neel Guha, Tatsunori Hashimoto, Peter Hen-  
534 derson, John Hewitt, Daniel E. Ho, Jenny Hong, Kyle Hsu, Jing Huang, Thomas F. Icard, Saahil  
535 Jain, Dan Jurafsky, Pratyusha Kalluri, Siddharth Karamcheti, Geoff Keeling, Fereshte Khani,  
536 O. Khattab, Pang Wei Koh, Mark S. Krass, Ranjay Krishna, Rohith Kuditipudi, Ananya Kumar,  
537 Faisal Ladhak, Mina Lee, Tony Lee, Jure Leskovec, Isabelle Levent, Xiang Lisa Li, Xuechen  
538 Li, Tengyu Ma, Ali Malik, Christopher D. Manning, Suvir P. Mirchandani, Eric Mitchell, Zanele  
539 Munyikwa, Suraj Nair, Avanika Narayan, Deepak Narayanan, Benjamin Newman, Allen Nie,  
Juan Carlos Niebles, Hamed Nilforoshan, J. F. Nyarko, Giray Ogut, Laurel Orr, Isabel Papadim-  
itriou, Joon Sung Park, Chris Piech, Eva Portelance, Christopher Potts, Aditi Raghunathan, Robert

540 Reich, Hongyu Ren, Frieda Rong, Yusuf H. Roohani, Camilo Ruiz, Jack Ryan, Christopher  
 541 R'e, Dorsa Sadigh, Shiori Sagawa, Keshav Santhanam, Andy Shih, Krishna Parasuram Srinivasan,  
 542 Alex Tamkin, Rohan Taori, Armin W. Thomas, Florian Tramèr, Rose E. Wang, William Wang,  
 543 Bohan Wu, Jiajun Wu, Yuhuai Wu, Sang Michael Xie, Michihiro Yasunaga, Jiaxuan You,  
 544 Matei A. Zaharia, Michael Zhang, Tianyi Zhang, Xikun Zhang, Yuhui Zhang, Lucia Zheng, Kaitlyn Zhou, and Percy Liang. On the opportunities and risks of foundation models. *ArXiv*, 2021.  
 545 URL <https://crfm.stanford.edu/assets/report.pdf>.

546

547 Elizabeth Bonawitz, Patrick Shafto, Hyowon Gweon, Noah D. Goodman, Elizabeth Spelke, and  
 548 Laura Schulz. The double-edged sword of pedagogy: Instruction limits spontaneous exploration  
 549 and discovery. *Cognition*, 120(3):322–330, 2011. ISSN 0010-0277. doi: <https://doi.org/10.1016/j.cognition.2010.10.001>. URL <https://www.sciencedirect.com/science/article/pii/S0010027710002258>. Probabilistic models of cognitive development.

550

551

552 Diana Borsa, André Barreto, John Quan, Daniel Jaymin Mankowitz, Rémi Munos, H. V. Hasselt, David Silver, and Tom Schaul. Universal successor features approximators. *ArXiv*,  
 553 abs/1812.07626, 2018. URL <https://api.semanticscholar.org/CorpusID:56475997>.

554

555

556 Michał Bortkiewicz, Władek Pałucki, Vivek Myers, Tadeusz Dziarmaga, Tomasz Arczewski, Łukasz Kuciński, and Benjamin Eysenbach. Accelerating Goal-Conditioned RL Algorithms and Research. In *International Conference on Learning Representations*, 2025. URL <https://arxiv.org/pdf/2408.11052.pdf>.

557

558

559

560

561 James Bradbury, Roy Frostig, Peter Hawkins, Matthew James Johnson, Chris Leary, Dougal Maclaurin, George Necula, Adam Paszke, Jake VanderPlas, Skye Wanderman-Milne, and Qiao Zhang. JAX: composable transformations of Python+NumPy programs, 2018. URL <https://github.com/jax-ml/jax>.

562

563

564

565 Greg Brockman, Vicki Cheung, Ludwig Pettersson, Jonas Schneider, John Schulman, Jie Tang, and Wojciech Zaremba. Openai gym. *ArXiv*, abs/1606.01540, 2016. URL <https://api.semanticscholar.org/CorpusID:16099293>.

566

567

568

569

570

571

572

573

574

575

576

577

578

579

580

581

582

583

584

585

586

587

588

589

590

591

592

593

Victor Campos, Alexander Trott, Caiming Xiong, Richard Socher, Xavier Giro-I-Nieto, and Jordi Torres. Explore, discover and learn: Unsupervised discovery of state-covering skills. In Hal Daumé III and Aarti Singh (eds.), *Proceedings of the 37th International Conference on Machine Learning*, volume 119 of *Proceedings of Machine Learning Research*, pp. 1317–1327. PMLR, 13–18 Jul 2020. URL <https://proceedings.mlr.press/v119/campos20a.html>.

Jiayu Chen, Dipesh Tamboli, Tian Lan, and Vaneet Aggarwal. Multi-task hierarchical adversarial inverse reinforcement learning. In *Proceedings of the 40th International Conference on Machine Learning*, ICML'23. JMLR.org, 2023.

Cheng Chi, Siyuan Feng, Yilun Du, Zhenjia Xu, Eric Cousineau, Benjamin Burchfiel, and Shuran Song. Diffusion policy: Visuomotor policy learning via action diffusion. In *Proceedings of Robotics: Science and Systems (RSS)*, 2023.

Cheng Chi, Zhenjia Xu, Siyuan Feng, Eric Cousineau, Yilun Du, Benjamin Burchfiel, Russ Tedrake, and Shuran Song. Diffusion policy: Visuomotor policy learning via action diffusion. *The International Journal of Robotics Research*, 2024.

Peter Dayan. Improving generalization for temporal difference learning: The successor representation. *Neural Comput.*, 5(4):613–624, July 1993. ISSN 0899-7667. doi: 10.1162/neco.1993.5.4.613. URL <https://doi.org/10.1162/neco.1993.5.4.613>.

Anca D. Dragan, Kenton C.T. Lee, and Siddhartha S. Srinivasa. Legibility and predictability of robot motion. In *Proceedings of the 8th ACM/IEEE International Conference on Human-Robot Interaction*, HRI '13, pp. 301–308. IEEE Press, 2013. ISBN 9781467330558.

Benjamin Eysenbach, Abhishek Gupta, Julian Ibarz, and Sergey Levine. Diversity is all you need: Learning skills without a reward function. *ArXiv*, abs/1802.06070, 2018. URL <https://api.semanticscholar.org/CorpusID:3521071>.

594 Benjamin Eysenbach, Xinyang Geng, Sergey Levine, and Ruslan Salakhutdinov. Rewriting history  
 595 with inverse rl: hindsight inference for policy improvement. In *Proceedings of the 34th Interna-*  
 596 *tional Conference on Neural Information Processing Systems*, NIPS '20, Red Hook, NY, USA,  
 597 2020. Curran Associates Inc. ISBN 9781713829546.

598 Benjamin Eysenbach, Ruslan Salakhutdinov, and Sergey Levine. The information geometry of  
 599 unsupervised reinforcement learning. *ArXiv*, abs/2110.02719, 2021. URL <https://api.semanticscholar.org/CorpusID:238408056>.

600 Benjamin Eysenbach, Tianjun Zhang, Sergey Levine, and Ruslan Salakhutdinov. Contrastive learn-  
 601 ing as goal-conditioned reinforcement learning. In *Proceedings of the 36th International Confer-*  
 602 *ence on Neural Information Processing Systems*, NIPS '22, Red Hook, NY, USA, 2022. Curran  
 603 Associates Inc. ISBN 9781713871088.

604 Chelsea Finn, Sergey Levine, and P. Abbeel. Guided cost learning: Deep inverse optimal control  
 605 via policy optimization. In *International Conference on Machine Learning*, 2016. URL <https://api.semanticscholar.org/CorpusID:8121626>.

606 Chelsea Finn, Tianhe Yu, Tianhao Zhang, Pieter Abbeel, and Sergey Levine. One-shot visual im-  
 607 itation learning via meta-learning. In Sergey Levine, Vincent Vanhoucke, and Ken Goldberg  
 608 (eds.), *Proceedings of the 1st Annual Conference on Robot Learning*, volume 78 of *Proceed-*  
 609 *ings of Machine Learning Research*, pp. 357–368. PMLR, 13–15 Nov 2017. URL <https://proceedings.mlr.press/v78/finn17a.html>.

610 Carlos Florensa, David Held, Xinyang Geng, and Pieter Abbeel. Automatic goal generation for  
 611 reinforcement learning agents. In Jennifer Dy and Andreas Krause (eds.), *Proceedings of the 35th*  
 612 *International Conference on Machine Learning*, volume 80 of *Proceedings of Machine Learning*  
 613 *Research*, pp. 1515–1528. PMLR, 10–15 Jul 2018. URL <https://proceedings.mlr.press/v80/florensa18a.html>.

614 C Daniel Freeman, Erik Frey, Anton Raichuk, Sertan Girgin, Igor Mordatch, and Olivier Bachem.  
 615 Brax – a differentiable physics engine for large scale rigid body simulation. *arXiv [cs.RO]*, June  
 616 2021.

617 Justin Fu, Katie Luo, and Sergey Levine. Learning robust rewards with adversarial inverse rein-  
 618 force learning. In *6th International Conference on Learning Representations, ICLR 2018,*  
 619 *Vancouver, BC, Canada, April 30 - May 3, 2018, Conference Track Proceedings*. OpenReview.net,  
 620 2018. URL <https://openreview.net/forum?id=rkHywl-A->.

621 Dibya Ghosh, Chethan Anand Bhateja, and Sergey Levine. Reinforcement learning from pas-  
 622 sive data via latent intentions. In Andreas Krause, Emma Brunskill, Kyunghyun Cho, Barbara  
 623 Engelhardt, Sivan Sabato, and Jonathan Scarlett (eds.), *Proceedings of the 40th International*  
 624 *Conference on Machine Learning*, volume 202 of *Proceedings of Machine Learning Research*,  
 625 pp. 11321–11339. PMLR, 23–29 Jul 2023. URL <https://proceedings.mlr.press/v202/ghosh23a.html>.

626 Alison Gopnik. Childhood as a solution to explore–exploit tensions. *Philosophical Transactions*  
 627 *of the Royal Society B: Biological Sciences*, 375(1803):20190502, 2020. doi: 10.1098/rstb.2019.  
 628 0502. URL <https://royalsocietypublishing.org/doi/abs/10.1098/rstb.2019.0502>.

629 Karol Gregor, Danilo Jimenez Rezende, and Daan Wierstra. Variational intrinsic con-  
 630 trol. *ArXiv*, abs/1611.07507, 2016. URL <https://api.semanticscholar.org/CorpusID:2918187>.

631 Hyowon Gweon and Laura Schulz. From exploration to instruction: Children learn from ex-  
 632 ploration and tailor their demonstrations to observers' goals and competence. *Child Develop-*  
 633 *ment*, 90(1):e148–e164, 2019. doi: <https://doi.org/10.1111/cdev.13059>. URL <https://srcd.onlinelibrary.wiley.com/doi/abs/10.1111/cdev.13059>.

634 Tuomas Haarnoja, Aurick Zhou, Pieter Abbeel, and Sergey Levine. Soft actor-critic: Off-policy  
 635 maximum entropy deep reinforcement learning with a stochastic actor. In *International confer-*  
 636 *ence on machine learning*, pp. 1861–1870. Pmlr, 2018.

648 Jonathan Ho and Stefano Ermon. Generative adversarial imitation learning. In *Proceedings of  
649 the 30th International Conference on Neural Information Processing Systems*, NIPS'16, pp.  
650 4572–4580, Red Hook, NY, USA, 2016. Curran Associates Inc. ISBN 9781510838819.  
651

652 Eric Jang, Alex Irpan, Mohi Khansari, Daniel Kappler, Frederik Ebert, Corey Lynch, Sergey Levine,  
653 and Chelsea Finn. BC-z: Zero-shot task generalization with robotic imitation learning. In *5th  
654 Annual Conference on Robot Learning*, 2021. URL [https://openreview.net/forum?  
655 id=8kbp23tSGYv](https://openreview.net/forum?id=8kbp23tSGYv).

656 Leslie Pack Kaelbling. Learning to achieve goals. In *International Joint Conference on Artificial In-  
657 telligence*, 1993. URL <https://api.semanticscholar.org/CorpusID:5538688>.  
658

659 Seongun Kim, Kyowoon Lee, and Jaesik Choi. Variational curriculum reinforcement learning for  
660 unsupervised discovery of skills. In *Proceedings of the 40th International Conference on Machine  
661 Learning*, ICML'23. JMLR.org, 2023.

662 Martin Klissarov and Marlos C. Machado. Deep laplacian-based options for temporally-extended  
663 exploration. In *Proceedings of the 40th International Conference on Machine Learning*, ICML'23.  
664 JMLR.org, 2023.  
665

666 Misha Laskin, Denis Yarats, Hao Liu, Kimin Lee, Albert Zhan, Kevin Lu, Catherine Cang,  
667 Lerrel Pinto, and Pieter Abbeel. Urlb: Unsupervised reinforcement learning bench-  
668 mark. In J. Vanschoren and S. Yeung (eds.), *Proceedings of the Neural Information  
669 Processing Systems Track on Datasets and Benchmarks*, volume 1, 2021. URL [https://datasets-benchmarks-proceedings.neurips.cc/paper\\_files/paper/2021/file/091d584fced301b442654dd8c23b3fc9-Paper-round2.pdf](https://datasets-benchmarks-proceedings.neurips.cc/paper_files/paper/2021/file/091d584fced301b442654dd8c23b3fc9-Paper-round2.pdf).  
670

671 Chen Ma, Dylan R. Ashley, Junfeng Wen, and Yoshua Bengio. Universal successor features  
672 for transfer reinforcement learning. *ArXiv*, abs/2001.04025, 2018. URL <https://api.semanticscholar.org/CorpusID:86513851>.  
673

674 Yecheng Jason Ma, Shagun Sodhani, Dinesh Jayaraman, Osbert Bastani, Vikash Kumar, and  
675 Amy Zhang. Vip: Towards universal visual reward and representation via value-implicit pre-  
676 training. *ArXiv*, abs/2210.00030, 2022. URL <https://api.semanticscholar.org/CorpusID:252683397>.  
677

678 Marlos C. Machado, Marc G. Bellemare, and Michael H. Bowling. A laplacian framework for option  
679 discovery in reinforcement learning. In Doina Precup and Yee Whye Teh (eds.), *Proceedings of  
680 the 34th International Conference on Machine Learning*, ICML 2017, Sydney, NSW, Australia,  
681 6–11 August 2017, volume 70 of *JMLR Workshop and Conference Proceedings*, pp. 2295–2304.  
682 JMLR.org, 2017. URL <http://proceedings.mlr.press/v70/machado17a.html>.  
683

684 Russell Mendonca, Oleh Rybkin, Kostas Daniilidis, Danijar Hafner, and Deepak Pathak.  
685 Discovering and achieving goals via world models. In M. Ranzato, A. Beygelzimer,  
686 Y. Dauphin, P.S. Liang, and J. Wortman Vaughan (eds.), *Advances in Neural In-  
687 formation Processing Systems*, volume 34, pp. 24379–24391. Curran Associates, Inc.,  
688 2021. URL [https://proceedings.neurips.cc/paper\\_files/paper/2021/file/cc4af25fa9d2d5c953496579b75f6f6c-Paper.pdf](https://proceedings.neurips.cc/paper_files/paper/2021/file/cc4af25fa9d2d5c953496579b75f6f6c-Paper.pdf).  
689

690 Vivek Myers, Chongyi Zheng, Anca Dragan, Sergey Levine, and Benjamin Eysenbach. Learn-  
691 ing Temporal Distances: Contrastive Successor Features Can Provide a Metric Structure for  
692 Decision-Making. In *International Conference on Machine Learning*, 2024. URL <https://proceedings.mlr.press/v235/myers24a.html>.  
693

694 Ashvin V Nair, Vitchyr Pong, Murtaza Dalal, Shikhar Bahl, Steven Lin, and Sergey  
695 Levine. Visual reinforcement learning with imagined goals. In S. Bengio, H. Wal-  
696 lach, H. Larochelle, K. Grauman, N. Cesa-Bianchi, and R. Garnett (eds.), *Ad-  
697 vances in Neural Information Processing Systems*, volume 31. Curran Associates, Inc.,  
698 2018. URL [https://proceedings.neurips.cc/paper\\_files/paper/2018/file/7ec69dd44416c46745f6edd947b470cd-Paper.pdf](https://proceedings.neurips.cc/paper_files/paper/2018/file/7ec69dd44416c46745f6edd947b470cd-Paper.pdf).  
699

702 Andrew Y. Ng and Stuart J. Russell. Algorithms for inverse reinforcement learning. In *Proceedings*  
 703 *of the Seventeenth International Conference on Machine Learning*, ICML '00, pp. 663–670, San  
 704 Francisco, CA, USA, 2000. Morgan Kaufmann Publishers Inc. ISBN 1558607072.

705 Octo Model Team, Dibya Ghosh, Homer Walke, Karl Pertsch, Kevin Black, Oier Mees, Sudeep  
 706 Dasari, Joey Hejna, Charles Xu, Jianlan Luo, Tobias Kreiman, You Liang Tan, Pannag Sanketi,  
 707 Quan Vuong, Ted Xiao, Dorsa Sadigh, Chelsea Finn, and Sergey Levine. Octo: An open-source  
 708 generalist robot policy. In *Proceedings of Robotics: Science and Systems*, Delft, Netherlands,  
 709 2024.

710 Aaron van den Oord, Yazhe Li, and Oriol Vinyals. Representation Learning with Contrastive Pre-  
 711 dictive Coding. *arXiv:1807.03748 [cs, stat]*, July 2018. URL <https://arxiv.org/abs/1807.03748>. arXiv: 1807.03748.

712 OpenAI OpenAI, Matthias Plappert, Raul Sampedro, Tao Xu, Ilge Akkaya, Vineet Kosaraju, Peter  
 713 Welinder, Ruben D'Sa, Arthur Petron, Henrique Pondé de Oliveira Pinto, Alex Paino, Hyeonwoo  
 714 Noh, Lilian Weng, Qiming Yuan, Casey Chu, and Wojciech Zaremba. Asymmetric self-play for  
 715 automatic goal discovery in robotic manipulation. *ArXiv*, abs/2101.04882, 2021. URL <https://api.semanticscholar.org/CorpusID:231592353>.

716 Seohong Park, Kimin Lee, Youngwoon Lee, and Pieter Abbeel. Controllability-aware unsuper-  
 717 vised skill discovery. In Andreas Krause, Emma Brunskill, Kyunghyun Cho, Barbara Engelhardt,  
 718 Sivan Sabato, and Jonathan Scarlett (eds.), *Proceedings of the 40th International Conference on  
 Machine Learning*, volume 202 of *Proceedings of Machine Learning Research*, pp. 27225–27245.  
 719 PMLR, 23–29 Jul 2023a. URL <https://proceedings.mlr.press/v202/park23h.html>.

720 Seohong Park, Oleh Rybkin, and Sergey Levine. Metra: Scalable unsupervised rl with metric-aware  
 721 abstraction. *ArXiv*, abs/2310.08887, 2023b. URL <https://api.semanticscholar.org/CorpusID:264128272>.

722 Deepak Pathak, Pulkit Agrawal, Alexei A. Efros, and Trevor Darrell. Curiosity-driven exploration  
 723 by self-supervised prediction. In Doina Precup and Yee Whye Teh (eds.), *Proceedings of the 34th  
 International Conference on Machine Learning*, volume 70 of *Proceedings of Machine Learning  
 Research*, pp. 2778–2787. PMLR, 06–11 Aug 2017. URL <https://proceedings.mlr.press/v70/pathak17a.html>.

724 Deepak Pathak, Parsa Mahmoudieh, Guanghao Luo, Pulkit Agrawal, Dian Chen, Fred Shentu, Evan  
 725 Shelhamer, Jitendra Malik, Alexei A. Efros, and Trevor Darrell. Zero-shot visual imitation. In  
 726 *2018 IEEE/CVF Conference on Computer Vision and Pattern Recognition Workshops (CVPRW)*,  
 727 pp. 2131–21313, 2018. doi: 10.1109/CVPRW.2018.00278.

728 Deepak Pathak, Dhiraj Gandhi, and Abhinav Gupta. Self-supervised exploration via disagreement.  
 729 In Kamalika Chaudhuri and Ruslan Salakhutdinov (eds.), *Proceedings of the 36th International  
 Conference on Machine Learning*, volume 97 of *Proceedings of Machine Learning Research*, pp.  
 730 5062–5071. PMLR, 09–15 Jun 2019. URL <https://proceedings.mlr.press/v97/pathak19a.html>.

731 Matteo Pirotta, Andrea Tirinzoni, Ahmed Touati, Alessandro Lazaric, and Yann Ollivier. Fast imita-  
 732 tion via behavior foundation models. In B. Kim, Y. Yue, S. Chaudhuri, K. Fragkiadaki, M. Khan,  
 733 and Y. Sun (eds.), *International Conference on Representation Learning*, volume 2024, pp.  
 734 12685–12724, 2024. URL [https://proceedings.iclr.cc/paper\\_files/paper/2024/file/370645ae400005f888e418f46b594539-Paper-Conference.pdf](https://proceedings.iclr.cc/paper_files/paper/2024/file/370645ae400005f888e418f46b594539-Paper-Conference.pdf).

735 Silviu Pitis, Harris Chan, Stephen Zhao, Bradly Stadie, and Jimmy Ba. Maximum entropy gain  
 736 exploration for long horizon multi-goal reinforcement learning. In *Proceedings of the 37th Inter-  
 737 national Conference on Machine Learning*, ICML'20. JMLR.org, 2020.

738 Francesco Poli, Marlene Meyer, Rogier B. Mars, and Sabine Hunnius. Exploration in 4-year-old  
 739 children is guided by learning progress and novelty. *Child Development*, 96(1):192–202, 2025.  
 740 doi: <https://doi.org/10.1111/cdev.14158>. URL <https://srcd.onlinelibrary.wiley.com/doi/abs/10.1111/cdev.14158>.

756 Dean A. Pomerleau. Alvinn: an autonomous land vehicle in a neural network. In *Proceedings of the*  
 757 *2nd International Conference on Neural Information Processing Systems*, NIPS'88, pp. 305–313,  
 758 Cambridge, MA, USA, 1988. MIT Press.

759

760 Vitchyr H. Pong, Murtaza Dalal, Steven Lin, Ashvin Nair, Shikhar Bahl, and Sergey Levine. Skew-  
 761 fit: state-covering self-supervised reinforcement learning. In *Proceedings of the 37th Interna-*  
 762 *tional Conference on Machine Learning*, ICML'20. JMLR.org, 2020.

763

764 Sai Rajeswar, Pietro Mazzaglia, Tim Verbelen, Alexandre Piché, B. Dhoedt, Aaron C. Courville,  
 765 and Alexandre Lacoste. Mastering the unsupervised reinforcement learning benchmark from  
 766 pixels. In *International Conference on Machine Learning*, 2022. URL <https://api.semanticscholar.org/CorpusID:258887708>.

767

768 Scott Reed, Konrad Zolna, Emilio Parisotto, Sergio Gomez Colmenarejo, Alexander Novikov,  
 769 Gabriel Barth-Maron, Mai Gimenez, Yury Sulsky, Jackie Kay, Jost Tobias Springenberg, Tom  
 770 Eccles, Jake Bruce, Ali Razavi, Ashley Edwards, Nicolas Heess, Yutian Chen, Raia Hadsell,  
 771 Oriol Vinyals, Mahyar Bordbar, and Nando de Freitas. A generalist agent. *arXiv [cs.AI]*, May  
 772 2022.

773

774 Stephane Ross, Geoffrey Gordon, and Drew Bagnell. A reduction of imitation learning and struc-  
 775 tured prediction to no-regret online learning. In Geoffrey Gordon, David Dunson, and Miroslav  
 776 Dudík (eds.), *Proceedings of the Fourteenth International Conference on Artificial Intelligence*  
 777 *and Statistics*, volume 15 of *Proceedings of Machine Learning Research*, pp. 627–635, Fort Laud-  
 778 erdale, FL, USA, 11–13 Apr 2011. PMLR. URL <https://proceedings.mlr.press/v15/ross11a.html>.

779

780 Tom Schaul, Daniel Horgan, Karol Gregor, and David Silver. Universal value function approxima-  
 781 tors. In Francis Bach and David Blei (eds.), *Proceedings of the 32nd International Conference*  
 782 *on Machine Learning*, volume 37 of *Proceedings of Machine Learning Research*, pp. 1312–1320,  
 783 Lille, France, 07–09 Jul 2015. PMLR. URL <https://proceedings.mlr.press/v37/schaul15.html>.

784

785 Seyed Kamyar Seyed Ghasemipour, Shixiang (Shane) Gu, and Richard Zemel. Smile: Scal-  
 786 able meta inverse reinforcement learning through context-conditional policies. In H. Wal-  
 787 lach, H. Larochelle, A. Beygelzimer, F. d'Alché-Buc, E. Fox, and R. Garnett (eds.), *Ad-*  
 788 *vances in Neural Information Processing Systems*, volume 32. Curran Associates, Inc.,  
 789 2019. URL [https://proceedings.neurips.cc/paper\\_files/paper/2019/file/2b8f621e9244cea5007bac8f5d50e476-Paper.pdf](https://proceedings.neurips.cc/paper_files/paper/2019/file/2b8f621e9244cea5007bac8f5d50e476-Paper.pdf).

790

791 Archit Sharma, Shixiang Shane Gu, Sergey Levine, Vikash Kumar, and Karol Hausman. Dynamics-  
 792 aware unsupervised discovery of skills. *ArXiv*, abs/1907.01657, 2019. URL <https://api.semanticscholar.org/CorpusID:195791369>.

793

794 Harshit S. Sikchi, Siddhant Agarwal, Pranaya Jajoo, Samyak Parajuli, Caleb Chuck, Max Rudolph,  
 795 Peter Stone, Amy Zhang, and Scott Niekum. Rlzero: Direct policy inference from language  
 796 without in-domain supervision. 2024. URL <https://api.semanticscholar.org/CorpusID:274597708>.

797

798 David Silver, Aja Huang, Chris J Maddison, Arthur Guez, Laurent Sifre, George van den Driessche,  
 799 Julian Schrittwieser, Ioannis Antonoglou, Veda Panneershelvam, Marc Lanctot, Sander Dieleman,  
 800 Dominik Grewe, John Nham, Nal Kalchbrenner, Ilya Sutskever, Timothy Lillicrap, Madeleine  
 801 Leach, Koray Kavukcuoglu, Thore Graepel, and Demis Hassabis. Mastering the game of go with  
 802 deep neural networks and tree search. *Nature*, 529(7587):484–489, January 2016.

803

804 Aimee E. Stahl and Lisa Feigenson. Observing the unexpected enhances infants' learning and  
 805 exploration. *Science*, 348(6230):91–94, 2015. doi: 10.1126/science.aaa3799. URL <https://www.science.org/doi/abs/10.1126/science.aaa3799>.

806

807

808 Ahmed Touati and Yann Ollivier. Learning one representation to optimize all rewards. In *Proceed-*  
 809 *ings of the 35th International Conference on Neural Information Processing Systems*, NIPS '21,  
 Red Hook, NY, USA, 2021. Curran Associates Inc. ISBN 9781713845393.

810 Ahmed Touati, Jérémie Rapin, and Yann Ollivier. Does zero-shot reinforcement learning ex-  
 811 ist? *ArXiv*, abs/2209.14935, 2022. URL <https://api.semanticscholar.org/CorpusID:252596234>.

812

813 Tongzhou Wang, Antonio Torralba, Phillip Isola, and Amy Zhang. Optimal goal-reaching rein-  
 814 force learning via quasimetric learning. In *International Conference on Machine Learning*.  
 815 PMLR, 2023.

816

817 Zizhao Wang, Jiaheng Hu, Caleb Chuck, Stephen Chen, Roberto Martín-Martín, Amy Zhang, Scott  
 818 Niekuum, and Peter Stone. Skild: unsupervised skill discovery guided by factor interactions. In  
 819 *Proceedings of the 38th International Conference on Neural Information Processing Systems*,  
 820 NIPS '24, Red Hook, NY, USA, 2024. Curran Associates Inc. ISBN 9798331314385.

821

822 David Warde-Farley, Tom Van de Wiele, Tejas Kulkarni, Catalin Ionescu, Steven Hansen, and  
 823 Volodymyr Mnih. Unsupervised control through non-parametric discriminative rewards. *arXiv*  
 824 [*cs.LG*], November 2018.

825

826 Yifan Wu, George Tucker, and Ofir Nachum. The laplacian in rl: Learning representations with  
 827 efficient approximations. *arXiv preprint arXiv:1810.04586*, 2018.

828

829 Peter R Wurman, Samuel Barrett, Kenta Kawamoto, James MacGlashan, Kaushik Subramanian,  
 830 Thomas J Walsh, Roberto Capobianco, Alisa Devlic, Franziska Eckert, Florian Fuchs, Leilani  
 831 Gilpin, Piyush Khandelwal, Varun Kompella, Haochih Lin, Patrick MacAlpine, Declan Oller,  
 832 Takuma Seno, Craig Sherstan, Michael D Thomure, Houmehr Aghabozorgi, Leon Barrett, Rory  
 833 Douglas, Dion Whitehead, Peter Dürr, Peter Stone, Michael Spranger, and Hiroaki Kitano. Out-  
 racing champion gran turismo drivers with deep reinforcement learning. *Nature*, 602(7896):223–  
 228, February 2022.

834

835 Lantao Yu, Tianhe Yu, Chelsea Finn, and Stefano Ermon. Meta-inverse reinforcement learning with  
 836 probabilistic context variables. In H. Wallach, H. Larochelle, A. Beygelzimer, F. d'Alché-Buc,  
 837 E. Fox, and R. Garnett (eds.), *Advances in Neural Information Processing Systems*, volume 32.  
 838 Curran Associates, Inc., 2019. URL [https://proceedings.neurips.cc/paper\\_files/paper/2019/file/30de24287a6d8f07b37c716ad51623a7-Paper.pdf](https://proceedings.neurips.cc/paper_files/paper/2019/file/30de24287a6d8f07b37c716ad51623a7-Paper.pdf).

839

840 Tianhe Yu, Chelsea Finn, Annie Xie, Sudeep Dasari, Tianhao Zhang, Pieter Abbeel, and Sergey  
 841 Levine. One-shot imitation from observing humans via domain-adaptive meta-learning. *arXiv*  
 842 [*cs.LG*], February 2018.

843

844 Tom Zahavy, Yannick Schroecker, Feryal M. P. Behbahani, Kate Baumli, Sebastian Flenner-  
 845 hag, Shaobo Hou, and Satinder Singh. Discovering policies with domino: Diversity opti-  
 846 mization maintaining near optimality. *ArXiv*, abs/2205.13521, 2022. URL <https://api.semanticscholar.org/CorpusID:249097488>.

847

848 Chongyi Zheng, Jens Tuyls, Joanne Peng, and Benjamin Eysenbach. Can a misl fly? analysis and  
 849 ingredients for mutual information skill learning. *arXiv preprint arXiv:2412.08021*, 2024.

850

851 Brian D Ziebart, Andrew L Maas, J Bagnell, and A Dey. Maximum entropy inverse reinforcement  
 852 learning. *National Conference on Artificial Intelligence*, pp. 1433–1438, July 2008.

853

854 Matthew Zurek, Andreea Bobu, Daniel S. Brown, and Anca D. Dragan. Situational confidence  
 855 assistance for lifelong shared autonomy. In *2021 IEEE International Conference on Robotics and  
 856 Automation (ICRA)*, pp. 2783–2789. IEEE Press, 2021. doi: 10.1109/ICRA48506.2021.9561839.  
 857 URL <https://doi.org/10.1109/ICRA48506.2021.9561839>.

## 858 A THEORETICAL ANALYSIS

### 859 A.1 CIRL IS CONSISTENT

860 *Proof.* MaxEnt IRL corresponds to the following objective:

$$863 \arg \min_{\theta} D_{\text{KL}}(p_{\pi_E(\tau)} \| p^*(\tau)) = \arg \max_{\theta} \mathbb{E}_{p_{\pi_E}(\tau)} [\log p^*(\tau)]$$

864 Under MaxEnt modeling, each goal  $g$  induces a trajectory model  $p^*(\tau \mid g) \propto$   
 865  $\left[ \rho_0(s_0) \prod_{t=0}^T p(s_{t+1} \mid s_t, a_t) \right] \exp \left( \sum_{t=0}^T r_g(s_t, a_t) \right)$  with log-partition  $\log Z_g$ . In a goal-  
 866 conditioned setting, taking the reward to be entirely determined by  $g$  means the family  $\{p^*(\tau \mid g)\}_g$   
 867 is indexed by goals, and the learning objective can be posed as minimizing the average forward KL  
 868

$$870 \min_{\theta} \mathbb{E}_{p(g)} [D_{\text{KL}}(p_E(\tau \mid g) \parallel p^*(\tau \mid g))],$$

872 where  $p(g)$  is the goal prior used both in data collection and modeling.

874 Define the expert and model joints over  $(\tau, g)$  as  $p_E(\tau, g) = p(g)p_E(\tau \mid g)$  and  $p^*(\tau, g) =$   
 875  $p(g)p^*(\tau \mid g)$ . When the same prior  $p(g)$  is used, the average conditional KL equals a joint for-  
 876 ward KL :

877

$$878 \mathbb{E}_{p(g)} [D_{\text{KL}}(p_E(\tau \mid g) \parallel p^*(\tau \mid g))] = \mathbb{E}_{p(g)} [D_{\text{KL}}(p_E(\tau, g) \parallel p^*(\tau, g))],$$

880 by applying Bayes Rule and canceling the identical priors.

881 Apply the KL chain rule to the joint KL:

882

$$884 D_{\text{KL}}(p_E(\tau, g) \parallel p^*(\tau, g)) = D_{\text{KL}}(p_E(\tau) \parallel p^*(\tau)) + \mathbb{E}_{\tau \sim p_E(\tau)} [D_{\text{KL}}(p_E(g \mid \tau) \parallel p^*(g \mid \tau))],$$

886 Thus our MaxEnt IRL objective is

887

$$889 \min_{\theta} \mathbb{E}_{p(g)} D_{\text{KL}}(p_E(\tau \mid g) \parallel p^*(\tau \mid g)) = \min_{\theta} \{ D_{\text{KL}}(p_E(\tau) \parallel p^*(\tau)) + \mathbb{E}_{p_E(\tau)} D_{\text{KL}}(p_E(g \mid \tau) \parallel p^*(g \mid \tau)) \} \quad (4)$$

892 Now we note that our marginal distribution  $p^*(\tau) = \int p(g)p^*(\tau \mid g)dg$  is a difficult integral to  
 893 compute and thus apply variational inference by introducing the amortized variational distribution  
 894  $q_{\xi}(g; \tau)$ . Then

895

$$896 \log p^*(\tau) = \text{ELBO}(\theta, \xi; \tau) + D_{\text{KL}}(q_{\xi}(g \mid \tau) \parallel p^*(g \mid \tau))$$

897 where

$$899 \text{ELBO} = \mathbb{E}_{q_{\xi}} [\log p(g) + \log p^*(\tau \mid g) - \log q_{\xi}(g \mid \tau)]$$

900 Taking the expectation over expert trajectories:

901

$$902 \min_{\theta} \{ D_{\text{KL}}(p_E(\tau) \parallel p^*(\tau)) \} = \max_{\theta} \mathbb{E}_{p_E(\tau)} [\log p^*(\tau)] \\ 903 = \max_{\xi} \mathbb{E}_{q_{\xi}} [\log p(g) + \log p^*(\tau \mid g) - \log q_{\xi}(g \mid \tau)] \\ 904 = \min_{\xi} [D_{\text{KL}}(q_{\xi}(g \mid \tau) \parallel p^*(g \mid \tau))]$$

905

906

907

908

909 Now we see the major issue with using the ELBO/reverse KL is that it requires us to be able to  
 910 evaluate the conditional likelihood  $p^*(\tau \mid g)$ . This is impossible in our scenario, but we could sample  
 911 from it since we can sample from the trajectory distribution of our MaxEnt RL policy. This motivates  
 912 the use of **Forward Amortized Variational Inference (FAVI)**, which uses the forward KL instead  
 913 of the reverse KL in its optimization (Ambrogioni et al., 2019).

914 The loss function of FAVI derives from the joint-contrastive variational inference objective and is  
 915 expressed as:

916

917

$$\mathcal{L}_{\text{FAVI}}[p, q] = D(p^*(g, \tau) \parallel q_{\xi}(g, \tau))$$

918 To approximate the intractable posterior  $p^*(g | \tau)$ , we factorize the variational joint as the product  
 919 of a variational posterior  $q_\xi(g | \tau)$  and a sampling distribution of the data:  
 920

$$921 \quad q_\xi(\tau, g) = q_\xi(g | \tau)k(\tau) \\ 922$$

923 Now we note:  
 924

$$926 \quad D_{KL}(p^*(\tau, g) \| q_\xi(\tau, g)) = \mathbb{E}_{p^*(\tau, g)} \left[ \log \frac{p^*(\tau, g)}{q_\xi(g | \tau)k(\tau)} \right] \quad (5) \\ 927$$

$$928 \quad = -\mathbb{E}_{p^*(\tau, g)} [\log q_\xi(g | \tau)] + \mathbb{E}_{p^*(\tau, g)} \left[ \log \frac{p^*(\tau, g)}{k(\tau)} \right] \quad (6) \\ 929 \\ 930$$

931 Considering only the terms that depends on  $q$ , we can define the FAVI loss as follows:  
 932

$$933 \quad \mathcal{L}_{\text{FAVI}} = -\mathbb{E}_{p^*(\tau, g)} [\log q_\xi(g | \tau)] \\ 934$$

935 This is precisely the loss function  $\mathcal{L}_{\text{Info}}(\xi)$  we train. Therefore, for our goal-conditioned setting,  
 936 the IRL problem can be reduced to one of learning a variational posterior with FAVI. Importantly,  
 937 note that the partition function is implicit within the samples we generate from the joint distribution  
 938 via  $g \sim p(g), \tau \sim p^*(\tau | g)$ , allowing us to consistently infer goals where methods that ignore the  
 939 partition function do not.  $\square$

## 940 A.2 FB IS INCONSISTENT

942 We prove this by providing a counterexample. The key idea in the counterexample is that an infre-  
 943 quently visited state may nonetheless be the policy's desired goal. We illustrate this with a simple  
 944 2-state MDP.  
 945

946 *Proof.* We define an MDP with 2 states  $(s_1, s_2)$  and 2 actions  $(a_1, a_2)$  with the following dynamics:  
 947

$$948 \quad p(s' | s, a) = \begin{cases} s_1, & \text{if } s = s_1, a = a_1 \\ s_1, & \text{w.p. } \frac{1}{2} \text{ if } s = s_1, a = a_2 \\ s_2, & \text{w.p. } \frac{1}{2} \text{ if } s = s_1, a = a_2 \\ s_2, & \text{if } s = s_2 \end{cases} \quad (7) \\ 949 \\ 950 \\ 951 \\ 952$$

953 Assume that the initial state is distributed  $p_0(s) = \mathbb{1}(s_1)$ . Note that state  $Y$  has just one action. The  
 954 only decision to make is the action at initial state  $X$ . Since all MDPs have deterministic optimal  
 955 policies, there are just two unique (potential) reward-maximizing policies for this MDP:  
 956

$$957 \quad \pi_1(a | s) = \begin{cases} a_1 & \text{if } s = s_1 \\ \text{any action} & \text{if } s = s_2 \end{cases} \quad (8) \\ 958$$

$$959 \quad \pi_2(a | s) = \begin{cases} a_2 & \text{if } s = s_1 \\ \text{any action} & \text{if } s = s_2 \end{cases} \quad (9) \\ 960$$

961 We will show that when data are collected from policy  $\pi_2$ , FB infers that data were collected with  
 962 policy  $\pi_1$ . This policy is clearly different, achieving different amounts of rewards (for all non-trivial  
 963 reward functions).

964 We next compute the occupancy measure for policy  $\pi_2$ . From the initial state  $x$ , the policy transitions  
 965 to state  $y$  with probability  $\frac{1}{2}$  at each time step. Thus, the probability of still being at state  $x$  after  $t$   
 966 time steps decays as  $1/2^t$ . The occupancy measure can thus be written as:  
 967

$$968 \quad \rho^{\pi_2}(s = X) = (1 - \gamma) + [1 + \gamma \frac{1}{2} + \gamma^2 \frac{1}{2^2} + \gamma^3 \frac{1}{2^3} + \dots] \\ 969 \quad = (1 - \gamma) \frac{1}{1 - \gamma/2} \quad (10)$$

$$970 \quad = (1 - \gamma) \sum_{t=0}^{\infty} (\gamma/2)^t = \frac{1 - \gamma}{1 - \gamma/2}. \quad (11) \\ 971$$

972 Then  $\rho^{\pi_2}(s = Y) = 1 - \rho^{\pi_2}(s = X)$ . Thus, when  $\gamma$  is small enough, policy  $\pi_2$  “spends more time  
973 at” state  $x$  than state  $y$ :

$$975 \quad \gamma < \frac{2}{3} \implies \rho^{\pi_2}(s = s_1) > \rho^{\pi_2}(s = s_2). \quad (12)$$

976 This will be a problem for FB, which infers rewards based not on the difficulty of maximizing them,  
977 but rather instead based on visitation counts:

$$979 \quad z_R = \sum_t B(s_t). \quad (13)$$

981 Without loss of generality, we assume that  $B(s_t) = \mathbb{1}(s_t)$ , a one hot vector; this solution is always  
982 admissible if the representations have high-enough dimension. Thus, the inferred reward function is

$$983 \quad r(s) = \begin{cases} \frac{1-\gamma}{1-\gamma/2} & \text{if } s = s_1 \\ \frac{\gamma/2}{1-\gamma/2} & \text{if } s = s_2 \end{cases} \quad (14)$$

986 Note that state  $s_1$  has a higher reward than state  $s_2$  with  $\gamma < \frac{2}{3}$ . Thus, the reward-maximizing policy  
987 for this reward function is  $\pi_1$  (which stays in  $s_1$ ), not  $\pi_2$  (which sometimes transitions to the lower  
988 reward state  $s_2$ ).  $\square$

989 This demonstrates that FB incorrectly identifies demonstrations from  $\pi_2$  as coming from  $\pi_1$ . The  
990 fundamental issue is that FB uses the occupancy measure directly as the reward signal without con-  
991 sidering the partition function or the policy’s optimality under that reward. This leads to systematic  
992 misidentification of the demonstrator’s true policy.

## 994 B ALGORITHM

997 We present pseudocode for training our zero-shot IL method based on contrastive RL pretraining:

---

### 999 Algorithm 1 Contrastive IRL

```
1000 1: Input: CRL loss  $\mathcal{L}_{\text{Critic}}$  and energy function  $f_{\phi, \psi}(s, a, g) = \phi(s, a)^T \psi(g)$  (Eysenbach et al.,  
1001 2022), Entropy-regularization value function  $\mathcal{L}_{\text{Entropy}}$ , actor objective  $\mathcal{L}_{\text{Actor}}$ , variational poste-  
1002 rior loss  $\mathcal{L}_{\text{info}}$   
1003 2: Initialize  $\phi, \psi, \theta, \xi, \pi$  and a pre-filled replay buffer  $\mathcal{D}$   
1004 3: repeat  
1005 4:   in parallel over environments  
1006 5:      $g = \arg \min_g \text{KDE}(\mathcal{D})$   
1007 6:     Store  $\tau \sim \pi(s, g)$  in  $\mathcal{D}$   
1008 7:   for  $j = 1, \dots, \text{num\_updates}$  do  
1009 8:     Randomly sample (with discount) a batch  $\mathcal{B}$  from  $\mathcal{D}$  of state-action pairs and  
1010       goals from their future  
1011 9:     Update critic:  
1012        $(\phi, \psi) \leftarrow (\phi, \psi) - \alpha \nabla_{\phi, \psi} [\mathcal{L}_{\text{Critic}}(\mathcal{B}; \phi, \psi)]$   
1013 10:    Update entropy-regularization value function:  
1014        $(\theta) \leftarrow (\theta) - \alpha \nabla_{\theta} [\mathcal{L}_{\text{Entropy}}(\mathcal{B}; \theta)]$   
1015 11:    Update policy:  
1016        $\pi \leftarrow \pi - \alpha \nabla_{\pi} [\mathcal{L}_{\text{Actor}}(\mathcal{B}; \phi, \psi, \pi)]$   
1017 12:    Update variational posterior:  
1018        $q \leftarrow q - \alpha \nabla_{\xi} [\mathcal{L}_{\text{Info}}(\mathcal{B}; \phi, \psi, \pi)]$   
1019 13: until convergence
```

---

## 1022 C EXPERIMENTAL DETAILS

1024 We ran our experiments building off the JaxGCRL benchmark (Bortkiewicz et al., 2025). Unless  
1025 otherwise mentioned, we used the same hyperparameters as that implementation.  $\alpha$  used for Maxi-  
mum Entropy IRL was 1e-5. For the FB representation, PSM and HILP baselines, we use the same

1026 encoder networks as in JaxGCRL and the same actor and critic learning rates. The metric value net  
 1027 for the HILP baseline similarly uses the JaxGCRL encoder architecture for the phi network. For  
 1028 the context encoder, we also use the JaxGCRL encoder and train to predict the mean and variance  
 1029 of a Gaussian. The backbone MLP of the JaxGCRL encoder networks has a hidden width of 256  
 1030 units, hidden depth of 2 layers, and 1 skip connection. We use the Swish activation after each hidden  
 1031 Dense layer. We used the seed 1 to train each type of policy.  
 1032

1033 Table 1: Reacher environment hyperparameters  
 1034

1035	hyperparameter	value
1036	batch size	1024
1037	num timesteps	20,000,000
1038	num environments	256

1042 Table 2: Pusher environment hyperparameters (goal: 3D position and 3D linear velocity)  
 1043

1044	hyperparameter	value
1045	batch size	256
1046	num timesteps	60,000,000
1047	num environments	512

1052 Table 3: Ant environment hyperparameters (goal: 2D position)  
 1053

1054	hyperparameter	value
1055	batch size	512
1056	num timesteps	30,000,000
1057	num environments	1024

1061 Table 4: Ant environment hyperparameters (goal: 3D position and 3D linear velocity)  
 1062

1063	hyperparameter	value
1064	batch size	256
1065	num timesteps	600,000,000
1066	num environments	512
1067	healthy z range	(0.0, 4.0)
1068	target z	Uniform over range (0.2, 2.0)
1069	target 3D linear velocity	Uniform over (-1.0, 1.0)

1073 Table 5: Ant environment hyperparameters (goal: 3D angular velocity)  
 1074

1075	hyperparameter	value
1076	batch size	256
1077	num timesteps	600,000,000
1078	num environments	512
1079	target 3D angular velocity	Uniform over (-2.5, 2.5)

1080  
1081  
1082 Table 6: PointMaze environment hyperparameters (goal: 2D position)  
1083  
1084  
1085  
1086  
1087  
1088  
1089

hyperparameter	value
batch size	1024
num environments	256
num timesteps	20,000,000 (U-Maze) 40,000,000 (Big Maze) 60,000,000 (Hardest Maze)

1090 C.1 ENVIRONMENTS  
1091

**Reacher:** This environment is a 2D manipulation task involving a two-jointed robotic arm. The goal is to move the arm’s end effector to a sampled 2-dimensional target located randomly within a workspace disk. The 11-dimensional state space includes joint angles and velocities along with the position of the end effector. The 2-dimensional action represents torques applied at the arm’s hinge joints.

**Pusher:** This features a 3D robotic arm and a movable object resting on a surface. The objective is to push the object into a 2D goal location randomly sampled at each episode reset. The 23-dimensional state space includes the arm’s joint angles, velocities, and the position of the movable object. The 7-dimensional action space controls the robotic arm via continuous motor torques at its joints.

**Ant:** This locomotion task involves a quadruped navigating towards target XY positions randomly sampled from a circle around its starting position. The 29-dimensional state space comprises the robot’s joint positions, orientations, and velocities, and the 8-dimensional action space consists of torques applied to each of the multiple leg joints. When using CIRL to infer URLB rewards, we expand the goal space to include the 3D position and 3D linear velocity or 3D angular velocity.

**PointMaze:** This navigation task involves a point mass navigating towards a target XY position in a constructed maze. The 4-dimensional state space includes the position and linear velocity of the point mass, and the 2D action space controls linear force along slide joints of the point mass in the environment. The possible configurations include U-Maze (20 x 20 maze layout), Big Maze (32 x 32 maze layout), and Hardest Maze (36 x 48 maze layout), in order of increasing state space size.

1127 D ADDITIONAL RESULTS  
1128

Figure 8 ablates CIRL performance against alternate goal inference methods: knowing the true goal or inferring the goal to be the last state of the expert demonstration. When we provide the true goal to a policy trained with CRL and GoalKDE exploration, we get a significant boost in imitation score, with any gap in imitation score from 100% likely due to distribution shift between

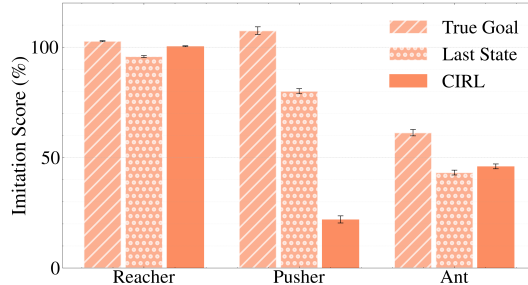


Figure 8: **Ablating CIRL.** For Pusher, most of the performance gap is due to goal inference, but for the Ant environment, most of the performance gap is likely due to distribution shift induced by GoalKDE.

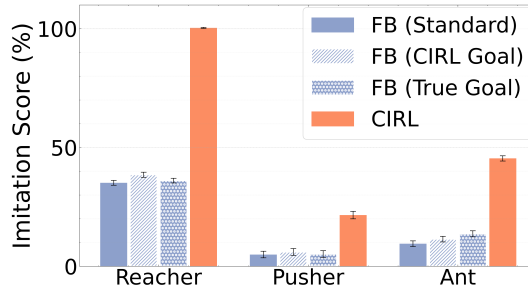


Figure 9: **Use the backward representation of the CIRL inferred goal to command the FB policy.** Comparing alternate methods of computing the FB latent against the standard FB baseline, CIRL still achieves higher imitation scores.

1134 goals sampled via GoalKDE and those from the oracle test distribution, and alternative methods for  
 1135 goal exploration are a promising area for future work in GCRL. For goal-conditioned expert poli-  
 1136 cies, inferring the last state to be the goal can be a strong baseline, but would fail when we try to  
 1137 imitate a task such as an Ant jumping.

1138 In Figure 9, we imagine if the FB representation  
 1139 had access to the CIRL mean field inferred  
 1140 goal. Using this state to compute a backward  
 1141 representation latent to command the FB poli-  
 1142 cies, FB is still not able to match the per-  
 1143 formance of CIRL. This is likely because FB  
 1144 must perform more exploration to learn a zero-shot  
 1145 policy for all possible rewards, including goal-  
 1146 reaching rewards, while CIRL has a smaller hy-  
 1147 pothesis space of rewards to explore and learn.  
 1148 However, we do note that FB with the inferred  
 1149 goal does outperform FB with the latent com-  
 1150 puted from either the last state of the demon-  
 1151 stration or the averaged backward representa-  
 1152 tion of all states in the demonstration.

1153 In Figure 10, we perform further analysis of  
 1154 GoalKDE’s capabilities across increasingly complex PointMaze environments, with U Maze having  
 1155 the smallest state space and Hardest Maze having the largest. We see that as the state space grows,  
 1156 the performance gap between GoalKDE and Oracle goal sampling widens.

1157  
 1158  
 1159  
 1160  
 1161  
 1162  
 1163  
 1164  
 1165  
 1166  
 1167  
 1168  
 1169  
 1170  
 1171  
 1172  
 1173  
 1174  
 1175  
 1176  
 1177  
 1178  
 1179  
 1180  
 1181  
 1182  
 1183  
 1184  
 1185  
 1186  
 1187

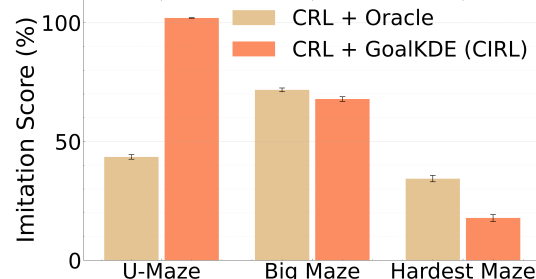


Figure 10: **Testing the limits of GoalKDE as a goal-sampling method for CIRL.** We see that the performance gap between CRL + Oracle and CIRL widens as the state space of PointMaze environments grows.